Eur. J. Biochem. **265**, 210–220 (1999) © FEBS 1999

Mutational analysis of Ser14 and Asp157 in the nucleotide-binding site of β-actin

Herwig Schüler[1], Elena Korenbaum[1]*, Clarence E. Schutt[2], Uno Lindberg[1] and Roger Karlsson[1]

[1]*Department of Cell Biology, The Wenner-Gren Institute, Stockholm University, Sweden;* [2]*The Henry Hoyt Laboratory, Department of Chemistry, Princeton University, NJ, USA*

This paper compares wild-type and two mutant β-actins, one in which Ser14 was replaced by a cysteine, and a second in which both Ser14 and Asp157 were exchanged (Ser14→Cys and Ser14→Cys,Asp157→Ala, respectively). Both of these residues are part of invariant sequences in the loops, which bind the ATP phosphates, in the interdomain cleft of actin. The increased nucleotide exchange rate, and the decreased thermal stability and affinity for DNase I seen with the mutant actins indicated that the mutations disturbed the interdomain coupling. Despite this, the two mutant actins retained their ATPase activity. In fact, the mutated actins expressed a significant ATPase activity even in the presence of Ca^{2+} ions, conditions under which actin normally has a very low ATPase activity. In the presence of Mg^{2+} ions, the ATPase activity of actin was decreased slightly by the mutations. The mutant actins polymerized as the wild-type protein in the presence of Mg^{2+} ions, but slower than the wild-type in a K^+/Ca^{2+} milieu. Profilin affected the lag phases and elongation rates during polymerization of the mutant and wild-type actins to the same extent, whereas at steady-state, the concentration of unpolymerized mutant actin appeared to be elevated. Decoration of mutant actin filaments with myosin subfragment 1 appeared to be normal, as did their movement in the low-load motility assay system. Our results show that Ser14 and Asp157 are key residues for interdomain communication, and that hydroxyl and carboxyl groups in positions 14 and 157, respectively, are not necessary for ATP hydrolysis in actin.

Keywords: ATP hydrolysis; β-actin mutants; polymerization; profilin; thermal stability.

Actin binds one mol of ATP and one divalent cation per mol of protein [1,2]. It is a Mg^{2+}-stimulated ATPase, but in low salt conditions, in which it does not polymerize, the ATPase activity is low. Under polymerizing conditions, the bound ATP is hydrolysed rather rapidly. It is currently believed that the actin monomers are incorporated into filaments in the ATP-state and that the nucleotide is hydrolysed to ADP.P_i only later. Subsequent release of P_i results in the final transformation of the actin monomers into the ADP-state of the classical helical filament. Although nucleotide hydrolysis can apparently be uncoupled from polymerization [3–6], it appears to be necessary for establishing a structural asymmetry between the two ends of the filament which may be important in the control of the *in vivo* recycling of subunits [7]. The actin ATPase has also been proposed to play a role in force generation by actomyosin [8].

The actin monomer consists of two major domains, each of which is divided into two subdomains (Fig. 1A) [9–12]. The nucleotide/cation complex is bound at the bottom of the cleft between the major domains with the adenine base resting in a hydrophobic pocket formed between subdomains 3 and 4. The polyphosphate tail is bound tightly by two invariant β-hairpin loops, Asn12–Cys17 and Asp154–His161, protruding into the interdomain cleft from subdomains 1 and 3, respectively (Fig. 1A,B). In the 'tight state' of the profilin/β-actin crystals [11], the β-phosphate is hydrogen bonded to the amide nitrogens of Ser14, Gly15 and Met16 in one of the loops and Asp157 in the other, and the γ-phosphate is bound to Ser14, Asp157, Gly158, and Val159. Thus both the β- and the γ-phosphates bridge the two loops. In the 'open state' [12], the relationship between the nucleotide and the phosphate-binding loops is slightly different. Here, the interactions with the subdomain 3 loop are weaker, leading to an increased exposure of the phosphate tail to the solvent as compared to the 'tight state'. By side chain interactions of Ser14 with Gly74, and of Asp157 with Arg183, both loops are linked with subdomains 2 and 4, respectively.

Formal analysis of the differences between the available actin structures have identified a shear region at the base of the central cleft of the actin monomer and provided a structural mechanism for domain rotations [13]. DNase I binds to subdomains 2 and 4, which in the actin filament are found at the slow-growing (–)-end (pointed end), clamping the major domains (Fig. 1A). Profilin binds to subdomains 1 and 3, i.e. at the (+)-end (barbed end). Both DNase I [14] and profilin [15–17] affect nucleotide binding in actin. Thus binding of DNase I or profilin is expected to fix the interdomain angle and restrict motions in the actin monomer [18]. As the interdomain contact is established *via* the nucleotide-binding site [19–23], mutations in the nucleotide-binding cleft could influence the binding constants for DNase I and profilin, respectively.

The mechanism of ATP hydrolysis by actin is unknown. A comparison of the 'open' and 'tight' states of the profilin-actin

Correspondence to U. Lindberg, Department of Cell Biology, The Wenner-Gren Institute, Stockholm University, S-106 91 Stockholm, Sweden. Fax: + 46 8 159837, Tel.: + 46 8 164101, E-mail: Uno.Lindberg@cellbio.su.se

Enzymes: deoxyribonuclease I (EC 3.1.21.1).

**Present address*: Institut für Biochemie I, Medizinische Fakultät der Universität Köln, D-50931 Köln, Germany.

(Received 7 June 1999, accepted 13 July 1999)

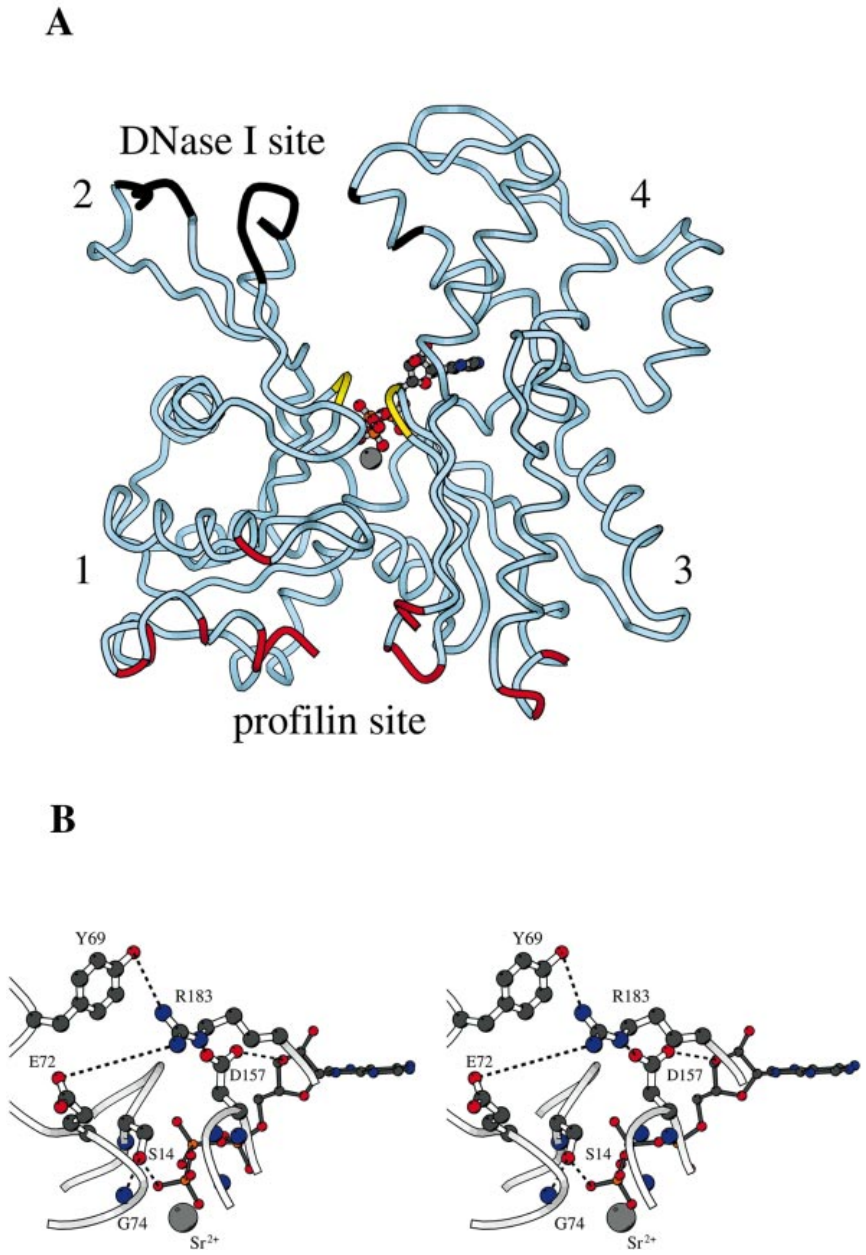

Fig. 1. Ribbon diagram representation of β-actin with bound ATP and Sr^{2+} [11] (A) and stereoview of the nucleotide-binding site (B). (A) The two highly conserved tripeptides in the phosphate-binding loops are shown in yellow. Residues involved in profilin binding are in red and residues involved in DNase I binding [9] are in black. Numbers indicate subdomains. (B) Residues Ser14 in subdomain 1, Tyr69, Glu72, and Gly74 in subdomain 2, Asp157 in subdomain 3, and Arg183 in subdomain 4 are indicated. The molecular representations were made in MOLSCRIPT (P. Kraulis, Avatar Software, Sweden).

crystal suggested that the nucleotide might become more tightly bound as polymerization proceeds, and that the residues involved in nucleophilic attack might become positioned as the polymer anneals [12]. The fact that the sequence Gly13-Ser14/Thr14-Gly15 is conserved, and that Asp157 likewise is part of an invariant tripeptide (Gly156-Asp157-Gly158) [24], emphasizes the importance of these residues in actin. It has been argued that the proximity [9] and the positioning of the hydroxyl of Ser14 relative to the γ-phosphate of ATP [25] suggest that it is the active-site nucleophile in the hydrolysis of the nucleotide and that it might be assisted by the carboxylate of Asp157. In the Hsc70 proteins, which have an ATP-binding fold similar to that of actin, the phosphate-binding loops are found to contain the same two tripeptides [26].

Mutational analysis of yeast actin demonstrated that Ser14 is crucial to the physiological functioning of actin, as replacing it with a cysteine or a glycine was lethal [27]. However, placing an alanine in this position caused only a temperature-sensitive phenotype [27], although such actin displayed several defects *in vitro* [28,29]. The double mutation Asp154→Ala,Asp157→Ala of yeast actin was also lethal [30].

Here, two mutant β-actins were expressed in the yeast *Saccharomyces cerevisiae*; one with a Ser14→Cys replacement and another in which both Ser14 and Asp157 were replaced (Ser14→Cys,Asp157→Ala). These actins were compared with yeast-expressed wild-type β-actin with respect to their DNase I-inhibiting activity, thermal stability, ATPase activity, and polymerizability. In addition, their interactions with profilin and myosin were studied. The results show that Ser14 and Asp157 are important for communication between the domains of the actin molecule. They also show that a thiol in position 14 and a methylene in position 157 do not interfere with the hydrolysis of ATP by actin. Part of this work has been presented in a short communication [31].

MATERIALS AND METHODS

Chemicals

Cyanogen bromide-activated Sepharose 4B was from Pharmacia Biotech. Bovine pancreatic DNase I (D-4527; Sigma) was used for affinity chromatography, and for the DNase I-inhibition assay the enzyme was from Boehringer Mannheim (grade I). DNase I from both sources was purified further by gel filtration [32]. Hydroxyapatite (even lot number) was from Clarkson Chromatography Products (South Williamsport, PA, USA). Rhodamine phalloidin, $1,N^6$-ethenoadenosine 5′-triphosphate (εATP) and *N*-(1-pyrene)iodoacetamide were from Molecular Probes (Eugene, OR, USA).

Mutagenesis and protein purification

Mutations were introduced in the chicken β-actin gene using the method described by Kunkel *et al*. [33]. The actin encoded by this gene is identical with bovine and human β-actin [24]. The wild-type and mutant β-actins were produced in *S. cerevisiae* using the temperature-inducible expression system described by Karlsson [34] and isolated by combining DNase I-affinity chromatography with chromatography on hydroxyapatite as in previous studies ([35] and references therein). Before formamide elution of the actin, yeast cofilin was removed from the DNase I-column with 0.5 M sodium acetate containing 0.5 mM ATP, 0.1 mM $CaCl_2$, pH 7.6 [36]. The actin was kept on ice in G-buffer (5 mM Tris/HCl pH 7.6, 0.5 mM ATP, 0.1 mM $CaCl_2$, 0.5 mM dithiothreitol, 0.006% NaN_3) and used within 1 week, or stored frozen as 25 μL droplets in liquid N_2. Protein concentrations were determined spectrophotometrically, using an extinction coefficient of $A_{290} = 0.63\ mL{\cdot}mg^{-1}{\cdot}cm^{-1}$ for G-actin [37]. Exchange of the high-affinity Ca^{2+} for Mg^{2+} was achieved by incubating actin in G-buffer with 0.2 mM EGTA and 50 μM $MgCl_2$ for 15 min at room temperature [38]. Profilin and β/γ-actin were purified from bovine thymus as described previously [39]. Rabbit skeletal muscle myosin was prepared according to Perry [40] with the addition of a final ultracentrifugation step.

Western blots

Pelleted yeast cells expressing recombinant β-actin (300 μL) were lysed by vigorous vortexing in the presence of an equal volume of glass beads and 100 μL G-buffer containing protease inhibitors [34] at 4 °C for 15 min. Cell debris was removed by low-speed centrifugation, and the low-salt lysate was centrifuged for 15 min at 180 000 ***g*** in a Beckman airfuge. The supernatant was adjusted to 2 mM $MgCl_2$, 50 mM KCl, and 100 μM phalloidin, and incubated for 1 h at room temperature, after which filamentous actin was collected by ultracentrifugation. The pelleted material was separated by SDS/PAGE [41], and the protein was electrotransferred to a nitrocellulose membrane (90 min, 50 mA). Monoclonal antibodies against β-actin (Sigma A-5316 [42]), and ECL-bioluminescence (Amersham, UK) were used for detection.

Copper binding

The intactness of the C terminus of the wild-type and mutant actins was assessed by determining their capacity to bind Cu^{2+} ions as described by Lehrer *et al*. [43]. Briefly, $CuCl_2$ (20 μM) was added under gentle stirring to a cuvette containing 10 μM actin, and the increase in absorbance at 350 nm was recorded using a Hewlett-Packard 8052A spectrophotometer. Freshly prepared β/γ-actin, intact and carboxypeptidase A-cleaved [44], was used as controls.

Nucleotide exchange

The time course of nucleotide exchange by monomeric actin was studied using εATP [45,46]. After removal of excess nucleotide by gel filtration, 0.1 mM εATP was immediately added to 13.5 μM actin, and the increase in the fluorescence on binding of εATP to actin was monitored using the Fluoroskan II plate reader as described above. When the signal had reached steady-state, 0.1 mM ATP was added and the signal decay was monitored to evaluate the rate of exit of εATP from the actin. The relative initial exchange rates were estimated by linear curve fitting using Microcal ORIGIN.

ATPase activity

Actin ATPase activity was determined essentially as described previously [47]. Briefly, actin in G-buffer was incubated with 33 nM (100 $\mu Ci{\cdot}\mu L^{-1}$) [γ-^{32}P]ATP overnight on ice. The ATPase activity of G-actin was then determined at 25, 30 and 37 °C, and of polymerizing actin at 25 °C. The amount of ATP hydrolysed was determined by taking aliquots of the incubation mixtures, extracting the inorganic phosphate with 0.3 M perchloric acid, precipitating the P_i by adding a mixture of triethylamine/HCl and ammonium molybdate, and capturing the precipitate on glass fiber filters (GF/F; Whatman). Dried filters were submerged in scintillation enhancer (Packard, USA) and counted in a Beckman LS 3801 scintillation counter.

DNase I-inhibition assay

Inhibition of DNase I by actin in G-buffer was measured as described earlier [48]. In the present experiments, the K_d for the actin/DNase I-interaction was determined from double-reciprocal plots of the dependence of DNase I-inhibition on actin concentration.

Thermal denaturation of actin

The thermal stability of actin was investigated by incubating the actin (6–8 μM) in G-buffer at 4 °C for 10 min. The temperature was then raised by 2 °C every 3 min, and the DNase I-inhibition activity of the sample was measured at the end of each 3-min period. The $T_{1/2}$ was defined as the temperature at which 50% of the DNase I-inhibition activity measured at 25 °C was lost. In the isothermal unfolding experiments, the loss of DNase I-inhibition activity was recorded at constant temperatures. The apparent first-order unfolding rate constants were determined by curve fitting, and the activation energies for the unfolding reactions were estimated from Arrhenius plots of those data [49].

Actin polymerization

The formation of actin filaments was followed by copolymerization with 2% pyrenyl-labelled β/γ-actin [50] at 25 °C monitoring the fluorescence increase at 410 nm (excitation wavelength, 365 nm) using a Fluoroskan II microplate reader (Labsystems, Finland). The reaction was induced by the addition of salt ($MgCl_2$ and/or KCl as indicated) to the protein solution (150 μL) in G-buffer. The elongation rates given

represent the highest slopes in the fluorescence increases, and the lag phases were determined by extrapolating these slopes to the background fluorescence levels. The concentration of nonsedimentable, DNase I-inhibiting actin at steady-state should represent the critical concentration of polymerization, [A_{cc}]. This was determined by pelleting the filaments by ultracentrifugation in a Beckman airfuge at 180 000 *g* for 20 min, and measuring the DNase I-inhibition activity in the supernatant [35,48]. However, as discussed below, conditions were found in which apparently considerable amounts of nonsedimentable, DNase I-inhibiting filaments or oligomers of actin were present.

Profilin interaction

The effect of profilin on the time course of actin polymerization was studied using the pyrenyl assay described above. Profilin and Mg–actin (8 μM each in G-buffer) were combined and preincubated for 5 min before addition of $MgCl_2$ to 1 mM and KCl to 100 mM. The effect of varying concentrations of profilin on the steady-state polymerization level of actin (6–8 μM) was studied by the sedimentation assay (described above) 3 h after addition of $MgCl_2$ (1 mM) and KCl (100 mM).

Motility assay

Wild-type and mutant β-actin was polymerized in 2 mM $MgCl_2$ and 100 mM KCl in the presence of rhodamine phalloidin at 1 : 1 molar ratio, and left on ice over night. The *in vitro* motility assay was performed in the presence of an oxygen-scavenging system [51,52].

RESULTS

Isolation of mutant actins

Wild-type, Ser14→Cys-, and Ser14→Cys,Asp157→Ala-β-actins were purified from extracts of yeast cells using DNase I-affinity chromatography, and separated from the yeast actin by chromatography on hydroxyapatite. Both mutant actins were eluted from the hydroxyapatite columns at a salt concentration close to that which displaced wild-type β-actin, suggesting that the surface structure of the mutant actins was not significantly altered [53]. The yield of wild-type actin was 7–8 mg and of the mutants 5–6 mg per 100 g of pelleted yeast cells. The lower yields of the mutant actins may reflect their decreased stability and/or lower affinity for DNase I (see below). Two other actins, carrying the mutations Ser14Δ and Ser14→Ala, respectively, were also expressed. The growth of the yeast cultures in these cases were similar to that seen with the other mutants suggesting that expression of the Ser14Δ- and Ser14→Ala-actins was not lethal to the yeast. The presence of these mutant actins in the yeast could be demonstrated by Western blot analysis of material pelleted from extracts treated with phalloidin, and with the use of antibodies to β-actin, suggesting that they formed filaments under these conditions. However, these mutant actins could not be isolated with the present method.

The C-terminus of actin is sensitive to proteolysis, and modifications in the C-terminal end of the protein are known to affect its activities [23,54]. To ensure that differences in the properties of the actins studied were not due to alterations of their C-termini, the actin preparations were analysed for their Cu^{2+}-binding properties. Yeast-expressed wild-type β-actin, double mutant Ser14→Cys,Asp157→Ala-actin, yeast actin, and bovine β/γ-actin all bound Cu^{2+} to the same extent, and in all cases the amount of Cu^{2+} bound was reduced by digesting the proteins with carboxypeptidase A. Also, actin containing the Cys374→Ser mutation [35] showed reduced Cu^{2+}-binding, confirming that this is a useful assay for changes at the

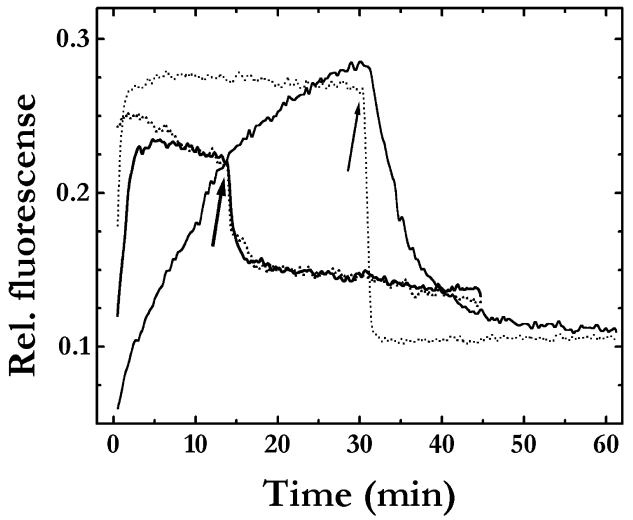

Fig. 2. Nucleotide exchange on wild-type and Ser14→Cys,Asp157→Ala-actin, measured using εATP. After addition of 100 μM εATP to 13.5 μM G-actin free of excess nucleotide, the fluorescence signal on binding of εATP was recorded. To follow the dissociation of the fluorescent nucleotide, 100 μM ATP was added at the time points indicated by arrows. The results obtained with single mutant Ser14→Cys-actin (data not shown) were virtually identical to those obtained with Ser14→Cys,Asp157→Ala-actin. The experiment was performed twice with each mutant and four times with wild-type actin. Thick lines, Mg-actins; thin lines, Ca-actins; solid lines, wild-type; dotted lines, Ser14→Cys,Asp157→Ala-actin.

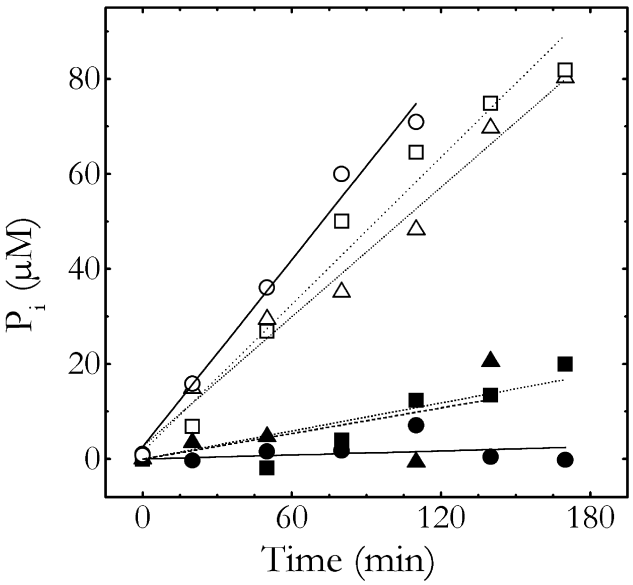

Fig. 3. Hydrolysis of ATP by wild-type and mutant G-actins. Time course of P_i generation at 30 °C determined with the use of [γ-^{32}P]ATP. Open symbols, Mg-actin; filled symbols, Ca-actin; circles and solid lines, wild-type actin; triangles and broken lines, Ser14Cy-actin; squares and dotted lines, Ser14→Cys,Asp157→Ala-actin. The ATPase rates are given in the text.

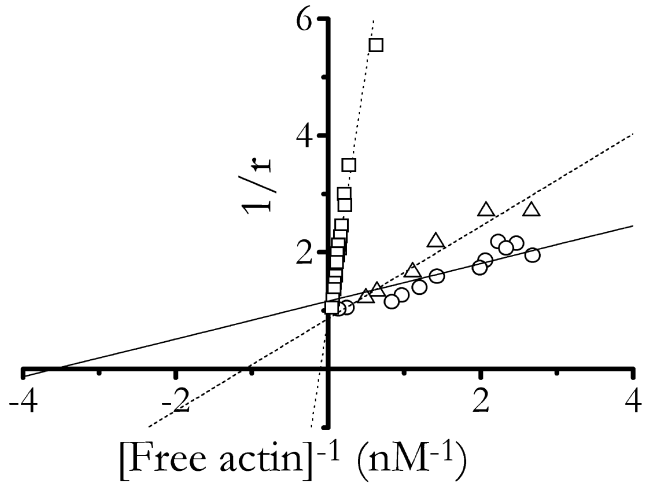

Fig. 4. Interaction of wild-type and mutant actins with DNase I. Double reciprocal plot of the dependence of DNase I inhibition on the concentration of wild-type (○), Ser14→Cys-(△) and Ser14→Cys,Asp157→Ala-actins (□). The dissociation constants determined from the intercepts with the abscissa were 0.28 nM for wild-type, 0.91 nM for Ser14→Cys-, and 9.8 nM for Ser14→Cys,Asp157→Ala-actin. The ratio of the concentrations of DNase I and bound actin, 1/*r*, is plotted on the ordinate.

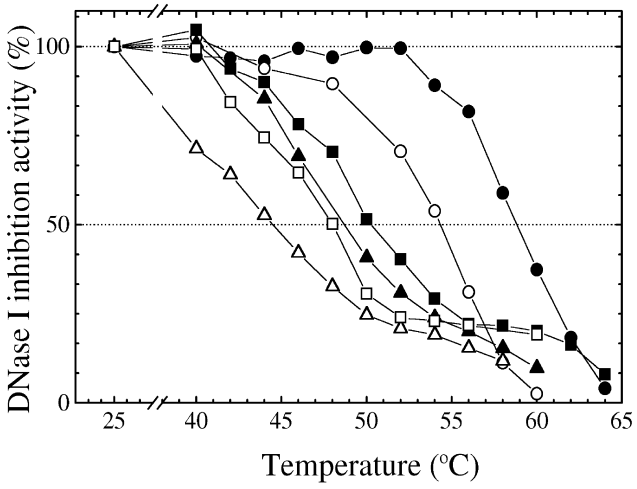

Fig. 5. Thermal stability of wild-type and mutant actins. Solutions of G-actin (6–8 μM) were heated at a rate of 40 °C·h^{-1} and their DNase I-inhibition activity was assessed at 3 min intervals. The curves represent DNase I-inhibition activities as a function of temperature, expressed as percentage of the values determined at 25 °C. Open symbols, Mg-actin; filled symbols, Ca-actin; circles, wild-type actin; triangles, Ser14→Cys-actin; squares, Ser14→Cys,Asp157→Ala-actin.

actin C-terminus [43]. Thus, differences observed in the properties of these actins should not be due to chemical alteration at the C-termini.

Nucleotide exchange

The amino acid residues replaced in the mutant actins are part of the two β-hairpin loops that bind tightly to the polyphosphate tail of ATP (Fig. 1). Therefore, it was of primary interest to find out whether the mutations had changed the nucleotide-binding properties of the protein. To do this 13.5 μM ATP-actin, from which excess ATP had been removed, was incubated with 100 μM εATP, and the increase in fluorescence resulting from the entry of εATP into the actin was monitored. As shown in Fig. 2, the exchange of ATP for εATP was 10 times faster with Ser14→Cys,Asp157→Ala-actin than with the wild-type protein, regardless of whether Mg^{2+} or Ca^{2+} was bound at the high-affinity cation binding site. After addition of 100 mM ATP, εATP was lost faster from Ser14→Cys, Asp157→Ala than from wild-type-Ca-actin, whereas there was no significant difference when the actins were in Mg^{2+}-bound form. With both wild-type and mutant actins, the nucleotide was exchanged faster when Mg^{2+} was present at the high affinity site. Similar results were obtained with Ser14→Cys-actin (data not shown). Thus, even though the interaction between the ATP phosphates primarily involves main chain amides, the exchange of serine for cysteine and aspartic acid for alanine increased nucleotide exchange. With the Mg-actins, the fluorescence signal progressively decreased from its maximal level, a phenomenon which was more pronounced with the mutants.

G-actin ATPase

Unpolymerized wild-type β-actin in the Ca^{2+}-form hydrolysed ATP at a very slow rate at 30 °C (≈ 0.05·h^{-1}). Compared to this, the mutant actins had 10 times higher activities (Fig. 3). In the Mg^{2+}-form, the actins had a much higher ATPase activity, although the mutant actins were somewhat less active than the wild-type (3.4·h^{-1}) under these conditions. Similar results were obtained when the ATPase activities of the wild-type and mutant actins were determined at 25 and 37 °C (data not shown). Thus, replacing Ser14 by a cysteine and Asp157 by an alanine did not abolish the ATPase activity.

DNase I-binding

The dissociation constants for the interactions between wild-type and mutant β-actins with DNase I were determined by

Table 1. Polymerization properties of wild-type and mutant β-actins. Lag phases and rates of polymer formation were determined from the experiments shown in Figs 6 and 7, and similar experiments, using pyrenyl fluorescence. FU, Relative fluorescense units.

		Lag phase (min)			Elongation rate (FU·min^{-1})		
Initial conditions	Polymerizing salts	Wild-type	S14C	S14C,D157A	Wild-type	S14C	S14C,D157→A
12 μM Ca-actin	0.1 M K^+	8.2	24	40	0.0015	0.0013	0.0009
12 μM Ca-actin	0.1 M K^+ + 1 mM EGTA	2.9	< 0.1	0.2	0.013	0.04	0.028
8 μM Mg-actin	1 mM Mg^{2+} + 0.1 M K^+	2.2	2.6	2.5	0.014	0.013	0.013
8 μM Mg-actin + 8 μM profilin	1 mM Mg^{2+} + 0.1 M K^+	9.7	8.7	10.0	0.0034	0.0038	0.0033

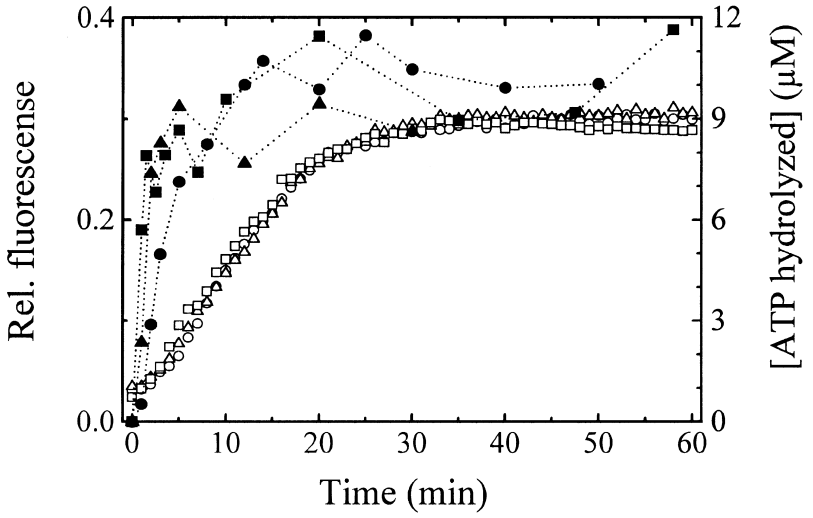

Fig. 6. Polymerization and ATP-hydrolysis of the wild-type and mutant actins. Polymerization of 8 μM Mg-actin initiated by 1 mM Mg^{2+} + 0.1 M K^+ was monitored using 2% pyrene-labelled β-actin (open symbols). Hydrolysis of ATP (filled symbols, dotted lines) was determined using [γ-^{32}P]ATP. Circles, wild-type actin; triangles, Ser14→Cys-actin; squares, Ser14→Cys,Asp157→Ala-actin.

studying DNase I inhibition as a function of actin concentration. From double-reciprocal plots of the data (Fig. 4), K_d values of 0.28, 0.91, and 9.8 nM were obtained for wild-type, Ser14→Cys-, and Ser14→Cys,Asp157→Ala-Ca-actins, respectively. Thus, mutations in the interdomain cleft of actin, and in particular the double mutation, affected the distantly located binding site for DNase I (Fig. 1A). The affinity for DNase I expressed by wild-type β-actin was similar to that determined previously for α-actin [14].

Thermal stability of actin monomers

The previous experiment suggested that the DNase I-inhibition assay is sensitive for changes in the interdomain relationship, and that it might be useful in the analysis of the conformational stability of actin. In the following experiments the stability of the actins at increasing temperatures was investigated. Wild-type β-actin lost its DNase I-inhibition activity in a single transition with a $T_{1/2}$ -value of 59 °C for the Ca^{2+}-bound form and of 54.5 °C for the Mg^{2+}-form as shown in Fig. 5. Also the Ser14→Cys- and Ser14→Cys,Asp157→Ala-actins were more stable with Ca^{2+} at the high-affinity divalent cation site, consistent with tighter binding of Ca-ATP. However, with the mutants, the loss of activity began at lower temperatures, and the transitions were biphasic and took place over a broader temperature range. An initial major decrease in the DNase I-binding activity was observed with $T_{1/2}$-values for Ser14→Cys,Asp157→Ala-actin of 50.2 °C with Ca^{2+} and of 48.6 °C with Mg^{2+} at the high affinity cation site; for Ser14→Cys-actin the corresponding values were 48.0 °C and 44.5 °C. At > 50 °C, the rate by which the activity was lost levelled off for the mutant actins. With the double mutant, there was a distinct plateau with 20–25% of the activity remaining until the temperature reached 59 °C after which the activity was rapidly lost.

The isothermal denaturation of the β-wild-type and Ser14→Cys,Asp157→Ala-actins with Mg^{2+} at their high-affinity cation sites was studied using DNase I inhibition. The wild-type actin denatured with apparent first-order kinetics, whereas the double mutant followed a more complex route (data not shown). This confirms that the unfolding reactions of the mutant actins were more complex than in the case of the wild-type protein as suggested by Fig. 5. The activation energies for the unfolding reactions, estimated from Arrhenius plots of the unfolding kinetics, were 248 kJ·mol^{-1} for wild-type and 102 kJ·mol^{-1} for double mutant actin. The wild-type value was similar to that determined previously for Ca-α-actin [55].

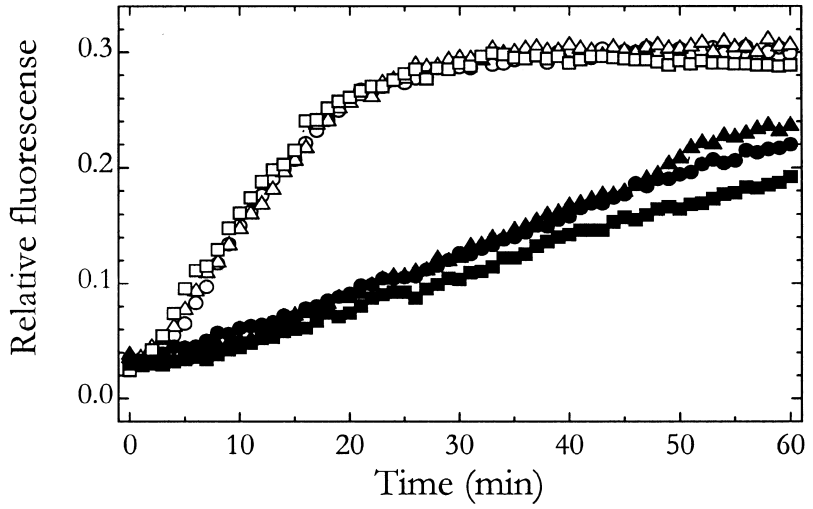

Fig. 7. Polymerization of wild-type and mutant actins in the presence of profilin. Profilin and Mg-actin (both 8 μM), including 2% pyrene-labelled β-actin, were preincubated for 5 min. Polymerization was initiated by 1 mM $MgCl_2$ + 100 mM KCl. Circles, wild-type actin; triangles, Ser14→Cys-actin; squares, Ser14→Cys,Asp157→Ala-actin; open symbols, absence of profilin; filled symbols, presence of equimolar amounts of profilin.

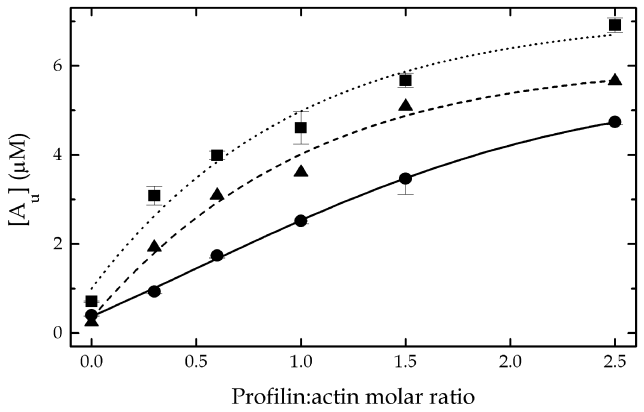

Fig. 8. Influence of profilin on the extent of filament formation of wild-type and mutant actins. The actins (8 μM; Mg-form) were polymerized with 1 mM $MgCl_2$ + 100 mM KCl in the presence of different concentrations of profilin. The concentrations of unpolymerized actin were determined after ultracentrifugation using the DNase I-inhibition assay. ●, Wild-type actin; ▲, Ser14→Cys-actin; ■, Ser14→Cys,Asp157→Ala-actin.

Actin polymerization

The polymerization kinetics of the two mutant actins differed significantly from those of the wild-type in K^+/Ca^{2+}-conditions. The lag phases were longer and the elongation rates were reduced (Table 1). As observed earlier for β-actin [35,56], removal of Ca^{2+} ions with EGTA had a dramatic effect on the polymerization of the actins. It shortened the lag phase, and accelerated the elongation for all three actins (Table 1). Under these conditions, the pyrenyl fluorescence signal increased approximately twice as fast with the mutants as compared to wild-type actin. On the other hand, the polymerization kinetics were unaffected by the mutations when filament formation was induced by 1 mM $MgCl_2$ + 0.1 M KCl (Fig. 6 and Table 1). Under these conditions, for all three actins, ATP hydrolysis preceded polymerization, and less than 20% of the actin was in polymer form by the time one molecule of ATP per actin had been hydrolysed (Fig. 6). In agreement with earlier observations (e.g. [57]), filament formation from Mg-actin was considerably faster than from Ca-actin.

The concentration of unpolymerized actin present at the steady-state of polymerization, $[A_{cc}]$, was estimated by sedimenting the actin filaments and determining the amount of actin in the supernatant using the DNase I-inhibition assay. Using this method, an $[A_{cc}]$ of 0.4 μM was obtained in Mg^{2+}-conditions for wild-type β-actin (Table 2). This agrees with the $[A_{cc}]$ values measured by steady-state dilutions of pyrenyl-labelled filamentous β-actin. The $[A_{cc}]$ for the single mutant was somewhat lower, whereas the double mutant actin polymerized less extensively than the wild-type. However, in the absence of Mg^{2+} ions the sedimentation/DNase I-inhibition assay detected elevated $[A_{cc}]$ values for the mutant actins. The extent of filament formation differed the most for Ser14→Cys, Asp157→Ala-actin, with an $[A_{cc}]$ of 5.6 μM, as compared to 2.1 μM for wild-type actin (Table 2). Thus, both the polymerization kinetics and the steady-state levels of polymerization were changed by the mutations in the absence of Mg^{2+} only.

The effect of profilin on the polymerization of wild-type and mutant actins was studied using the pyrenyl assay. Mixtures of Mg-actin and profilin (8 μM each) were preincubated for 5 min before polymerization was initiated by the addition of 1 mM $MgCl_2$ and 100 mM KCl. Under these conditions, both mutants polymerized with kinetics similar to those of wild-type actin (Fig. 7 and Table 1). Profilin prolonged the nucleation phase in the polymerization of wild-type actin from approximately 2 to 10 min and decreased the rate of polymer elongation by a factor of four. Profilin had the same effect on the polymerization of the mutant actins.

The steady-state level of unpolymerized actin, $[A_u]$, measured in the presence of increasing concentrations of profilin is shown in Fig. 8. Here, the different actins (8 μM, in the Mg-form) were incubated with increasing concentrations of profilin for 5 min, after which polymerizing salts were added (1 mM $MgCl_2$ + 100 mM KCl). After 3 h, the mixtures were centrifuged to sediment formed filaments, and the DNase I-inhibition activities in the supernatants were determined. The $[A_u]$ increased with increasing concentration of profilin, and for wild-type actin and profilin in equimolar amounts (Table 2), it was 2.5 μM ($[A_{cc}]$ of 0.4 μM in the absence of profilin). This apparent sequestering effect of profilin was more pronounced with the mutant actins. The concentrations of unpolymerized Ser14→Cys-and Ser14→Cys, Asp157→Ala-actin found in the supernatants increased from 0.25 to 3.6 μM and from 0.71 to 4.6 μM, respectively, when equimolar profilin was added. This was unexpected as the pyrenyl-assay indicated that all three actins had formed filaments to about the same extent (Fig. 7). Thus, in the case of the mutant actins only a fraction of the filamentous actin could be pelleted by ultracentrifugation. Instead, a large

Table 2. Steady-state critical concentrations for polymerization of wild-type and mutant β-actins under various salt conditions ($[A_{cc}]$) and in the presence of profilin ($[A_u]$). The values were determined by the sedimentation/DNase I-inhibition assay, and are given as means ± SD of 5–30 individual determinations using several preparations of yeast-expressed β-actin. Actin solutions (8 μM) were incubated for 3–5 h prior to the determination. Independent *t*-tests were run on all experimental data (values of $P < 0.01$ indicate a significant difference between wild-type and mutant).

		$[A_{cc}]$ (μM)		
Initial conditions	Polymerizing salts	Wild-type	Ser14→Cys	Ser14→Cys,Asp157→Ala
Ca-actin	100 mM KCl	2.1 ± 0.31	4.4 ± 0.54 ($P < 0.001$)	5.6 ± 0.29 ($P < 0.001$)
Ca-actin	100 mM KCl + 1 mM EGTA	0.29 ± 0.08	0.57 ± 0.116 ($P < 0.001$)	0.38 ± 0.226 ($P = 0.16$)
Mg-actin	1 mM $MgCl_2$/100 mM KCl	0.4 ± 0.02	0.25 ± 0.008 ($P < 0.001$)	0.71 ± 0.014 ($P < 0.001$)
Mg-actin + profilin (8 μM)	1 mM $MgCl_2$/100 mM KCl	2.52 ± 0.07	3.61 ± 0.12 ($P < 0.001$)	4.61 ± 0.37 ($P < 0.001$)

fraction of the actin was recovered in the supernatant and inhibited DNase I.

Myosin interaction

Myosin S1-decoration of wild-type and mutant actin filaments resulted in similar arrowhead patterns, and their translocation velocities in the *in vitro* motility assay did not differ from each other (data not shown). Thus the interaction with myosin was not dramatically affected by the introduced mutations.

DISCUSSION

Interdomain coupling in actin

In this paper we have addressed the role of Ser14 and Asp157 in the phosphate-binding loops of actin. The binding of the ATP phosphoryl oxygens to main chain amides in these β-hairpin loops (Fig. 1) stabilizes their strained conformations [25]. This allows additional bonds to form between loop residues and adjacent parts of subdomains 1 and 3 of the protein (Gly13 to Ser33, and Asp157 to Arg183). Through this extensive interdomain coupling, the monomer is held in a stable conformation. Any disturbance in the nucleotide-mediated interdomain coupling is expected to result in increased flexibility in the shear region connecting the two domains and in decreased stability.

DNase I connects the two domains at the (–)-end of the molecule, far away from the nucleotide-binding site. Thus, the DNase I-inhibiting activity of actin should be sensitive to changes in the interdomain relationship. This was corroborated by the decrease in DNase I-inhibition activity caused by the mutations in the phosphate-binding loops. The initial loss of DNase I-binding activity during thermal denaturation of the wild-type and mutant actins is interpreted as a breakdown of the interdomain coupling with retention of some DNase I-binding activity of either subdomain 2 or 4 (Fig. 1A). Then, complete loss of DNase I-inhibition activity would reflect a more extensive loss of structure. A disturbed interdomain relationship in the mutant actins was also found by nucleotide exchange experiments (Fig. 2). In addition to an apparently faster exchange of the bound nucleotide, the mutant actins displayed a prominent decrease in εATP fluorescence after first having reached a maximum level. This might indicate a secondary structural rearrangement. A similar loss of fluorescence has been observed for ADP-actin [58,59].

Ser14 is the only subdomain 1 residue which is within hydrogen bonding distance to both the γ-phosphate of ATP and a residue in subdomain 2 (Gly74 amide). Thus, the introduction of a cysteine, with its lower hydrogen bonding capacity [60] could influence the relative positioning and/or structure of subdomain 2 (Fig. 1), and cause the observed decrease in both thermal stability and affinity for DNase I of the mutant proteins. The larger volume of the cysteine compared to the serine (106 $Å^3$ versus 99 $Å^3$, [61]); can hardly explain the destabilizing effect on the structure, as a mutant of yeast actin with a threonine (122 $Å^3$) in position 14 is fully functional [27].

Likewise, Asp157 is important for the stability of the actin in that it provides a link to subdomain 4 (Fig. 1). Its amide nitrogen can be hydrogen bonded to oxygen atoms of the nucleotide phosphate tail, and its carboxylate is within hydrogen bonding distance of the ribose moiety. The carboxylate may also participate in a salt cluster with a guanidino nitrogen of Arg183. Other residues contributing to this salt cluster are Tyr69 and Glu72 in subdomain 2. Thus, through the side chain of Asp157, the phosphate-binding loop of subdomain 3 is linked both to the nucleotide and to residues in subdomains 2 and 4. Therefore, replacing Asp157 with an alanine was expected to increase the disturbance of the interdomain coupling causing even more pronounced effects on the properties of actin. That this was indeed the case was shown by a 30-fold increase in the K_d for DNase I.

Actin ATPase

The proximity and orientation of Ser14 relative to the ATP γ-phosphate, and the finding that replacing this residue with a cysteine is lethal in yeast [27] could be taken as an indication that this residue provides the nucleophile in the mechanism of ATP hydrolysis by actin [25]. The present work, however, shows that the Ser14→Cys and Ser14→Cys,Asp157→Ala mutants hydrolyse ATP at almost undiminished rates, and that hydrolysis occurs even under conditions where the wild-type protein is virtually inactive. Thus, either Ser14 is not the active-site nucleophile, or cysteine can function in its place. In the active site of certain phosphoryl transferases a cysteine appears to be of central importance to the reaction mechanism [62–65]. If cysteine can replace serine as a nucleophile in ATP hydrolysis in actin, the question remains why cysteine in this position is lethal and alanine is not [27]. Asp157 in actin has been proposed to act as an activator of the putative Ser14 nucleophile [25]. However, as shown here Asp157 can be replaced by an alanine without change in the ATPase activity of the actin. In myosin a serine has been suggested to coordinate an active water molecule without itself directly taking part in the cleavage of ATP [66]. A similar scenario in actin would explain the reduced hydrolytic activity observed with the Mg^{2+}-form of Ser14→Cys-actin, since cystidyls are poor hydrogen bonders [60]. The observation that yeast Ser14Ala-actin had a greatly reduced ATPase activity [28] agrees with this. However, since those experiments were conducted close to the melting temperature of the mutant actin, the results could have a different explanation. Unfortunately it has not been possible to purify β-actin having alanine in position 14 using our standard isolation procedure.

A different mechanism of ATP hydrolysis in the actin-fold family of proteins is suggested by recent analyses of the heat shock cognate protein, Hsc70. Here, a Mg^{2+}-ion and a lysine (Lys71) have proven essential for ATP hydrolysis [67], and two K^+ ions have been found in the active site [68]. In the proposed mechanism, Lys71 stabilizes a water molecule or a hydroxyl ion for nucleophilic attack on the γ-phosphate of ATP [67]. The similarity in the arrangement of certain amino acid residues surrounding the nucleotide and the divalent cation in actin could mean that actin operates in a similar way, and a prediction would be that Arg177 is involved in ATP hydrolysis in actin. Arginines or lysines have been found to stabilize the transition state of nucleotide hydrolysis in P-loop proteins including myosin and the rho-family of GTPases (reviewed in [69–71]). Moreover, a positively charged residue is necessary for phosphoryl transfer in CheY [72] and in other phosphoryl transferases. Thus, in the physiological structure of actin with Mg^{2+} at the high affinity site, a charged side chain may be similarly positioned to stabilize the negatively charged reactive intermediate.

Polymerization

Growth of actin filaments takes place preferentially at their (+)-end, i.e. actin monomers are added with their (–)-end

onto the (+)-end of a nucleus or preexisting filament. In the experiments presented in Table 1, presence of Ca^{2+} ions generally slowed down the polymerization of the actins. Similar effects have been seen previously [35,56,73]. In the K^+/Ca^{2+}-milieu, the mutant actins polymerized more slowly than wild-type actin, but faster than the wild-type when Ca^{2+} had been removed with EGTA. Thus, the mutant actins were changed in their polymerization characteristics, but the direction of change depended on the ionic conditions.

The MgATP-conformation of the actin monomer facilitates polymerization. Once the monomer is incorporated into a filament, nucleotide hydrolysis and phosphate release allow the monomer to attain a new conformation stabilized by the monomer–monomer interactions characteristic of the helical filament. Here, hydrolysis of ATP preceded filament formation during Mg^{2+}-induced polymerization of Mg-actins. The apparent uncoupling of the ATPase from filament elongation under nonseeded conditions seen here is unlike the situation in seeded α-actin solutions, in which ATP hydrolysis was found to lag behind filament elongation ([7], and references therein). This suggests a role of the actin ATPase during the nucleation phase primarily, and further studies are required for a full characterization of this process.

The concentrations of unpolymerized actin, $[A_{cc}]$, measured at steady-state of polymerization using the sedimentation/DNase-inhibition assay, under Mg^{2+}-conditions was close to the critical concentration of polymerization reported earlier for α- and β-actin [17,35]. However, in the profilin experiment, the pyrenyl assay indicated a rather high degree of polymer formation, whereas considerably lower concentrations of F-actin were detected by the sedimentation/DNase-inhibition assay. This is interesting, because actin filaments formed under physiological salt conditions have a rather low specific DNase-I-inhibiting activity, which is thought to result from actin monomers dissociating from the ends of the polymer, not to the binding of DNase I along the filaments [48]. In the present experiments, however, the actin oligomers or filament fragments formed under these conditions inhibited DNase I with high specific activity, suggesting that the DNase I interacted directly with the polymerized product. This is supported by electron microscopic observations of DNase I-induced changes along the length of actin filaments resulting in severing as part of the depolymerization process [74]. In the case of the mutant actins, due to changes in the interdomain relationship, the DNase I-binding site of the actin molecule in the filament might be more exposed. This is supported further by the altered conformation of yeast Ser14Ala-actin filaments [28,29].

ACKNOWLEDGEMENTS

The authors thank T. Hult for technical assistance, R. Page for help with MOLSCRIPT, and P. Nordlund for making us aware of the role of active-site cysteines in phosphoryl transfer reactions. This work was supported by grants to U. L. and R. K. from the Swedish Cancer Society and to C. E. S. from the NIH (GM44038).

REFERENCES

1. Asakura, S. (1961) The interaction between G-actin and ATP. *Arch. Biochem. Biophys.* **92**, 140–149.
2. Strohman, R.C. & Samorodin, A.J. (1962) The requirements for adenosine triphosphate binding to globular actin. *J. Biol. Chem.* **237**, 363–370.
3. Higashi. S. & Oosawa, F. (1965) Conformational changes associated with polymerization and nucleotide binding in actin molecules. *J. Mol. Biol.* **12**, 843–865.
4. Cooke, R. & Murdoch, L. (1973) Interaction of actin with analogs of adenosine triphosphate. *Biochemistry* **12**, 3927–3932.
5. Pardee, J. & Spudich, J.A. (1982) Mechanism of K^+-induced actin assembly. *J. Cell Biol.* **93**, 648–654.
6. Carlier, M.-F., Pantaloni, D. & Korn, E.D. (1984) Evidence for an ATP cap at the ends of actin filaments and its regulation of the F-actin steady state. *J. Biol. Chem.* **259**, 9983–9986.
7. Korn, E.D., Carlier, M.-F. & Pantaloni, D. (1987) Actin polymerization and ATP hydrolysis. *Science* **238**, 638–644.
8. Schutt, C.E. & Lindberg, U. (1998) Muscle contraction as a Markov process I: energetics of the process. *Acta Physiol. Scand.* **163**, 307–324.
9. Kabsch, W., Mannherz, H.G., Suck, D., Pai, E.F. & Holmes, K.C. (1990) Atomic structure of the actin: DNase I complex. *Nature* **347**, 37–44.
10. McLaughlin, P.J., Gooch, J.T., Mannherz, H.G. & Weeds, A.G. (1993) Structure of gelsolin segment 1-actin complex and the mechanism of filament severing. *Nature* **364**, 685–692.
11. Schutt, C.E., Myslik, J.C., Rozycki, M.D., Goonesekere, N.C.W. & Lindberg, U. (1993) The structure of crystalline profilin-beta-actin. *Nature* **365**, 810–816.
12. Chik, J.K., Lindberg, U. & Schutt, C.E. (1996) The structure of an open state of beta-actin at 2.65 Å resolution. *J. Mol. Biol.* **263**, 607–623.
13. Page, R., Lindberg, U. & Schutt, C.E. (1998) Domain motions in actin. *J. Mol. Biol.* **280**, 463–474.
14. Mannherz, H.G., Goody, R.S., Konrad, M. & Nowak, E. (1980) The interaction of bovine pancreatic deoxyribonuclease I and skeletal muscle actin. *Eur. J. Biochem.* **104**, 367–379.
15. Mockrin, S.C. & Korn, E.D. (1980) Acanthamoeba profilin interacts with G-actin to increase the rate of exchange of actin-bound adenosine 5′-triphosphate. *Biochemistry* **19**, 5359–5362.
16. Goldschmidt-Clermont, P.J., Machesky, L.M., Doberstein, S.K. & Pollard, T.D. (1991) Mechanism of the interaction of human platelet profilin with actin. *J. Cell Biol.* **113**, 1081–1089.
17. Korenbaum, E., Nordberg, P., Björkegren-Sjögren, C., Schutt, C.E., Lindberg, U. & Karlsson, R. (1998) The role of profilin in actin polymerization and nucleotide exchange. *Biochemistry* **37**, 9274–9283.
18. Rozycki, M.D., Myslik, J.C., Schutt, C.E. & Lindberg, U. (1994) Structural aspects of actin-binding proteins. *Curr. Opin. Cell Biol.* **6**, 87–95.
19. Frieden, C., Lieberman, D. & Gilbert, H.R. (1980) A fluorescent probe for conformational changes in skeletal muscle G-actin. *J. Biol. Chem.* **255**, 8991–8993.
20. Frieden, C. & Patane, K. (1985) Differences in G-actin containing bound ATP or ADP: the Mg^{2+}-induced conformational change requires ATP. *Biochemistry* **24**, 4192–4196.
21. Crosbie, R.H., Miller, C., Cheung, P., Goodnight, T., Muhlrad, A. & Reisler, E. (1994) Structural connectivity in actin: effect of C-terminal modifications on the properties of actin. *Biophys. J.* **67**, 1957–1964.
22. Muhlrad, A., Cheung, P., Phan, B.C., Miller, C. & Reisler, E. (1994) Dynamic properties of actin. Structural changes induced by beryllium fluoride. *J. Biol. Chem.* **269**, 11852–11858.
23. Strzelecka-Golaszewska. H., Mossakowska, M., Wozniak, A., Moraczewska, J. & Nakayama, H. (1995) Long-range conformational effects of proteolytic removal of the last three residues of actin. *Biochem. J.* **307**, 527–534.
24. Sheterline, P., Clayton, J. & Sparrow, J. (1996) Actin. *Protein Profile* **3**, 1–116.
25. Myslik, J.C. (1992) *The structure of actin in the crystalline profilin:actin complex.* Ph.D. Thesis, Princeton University.
26. Flaherty, K.M., McKay, D.B., Kabsch, W. & Holmes. K.C. (1991) Similarity of the three-dimensional structures of actin and the ATPase fragment of a 70-kDa heat shock cognate protein. *Proc. Natl Acad. Sci. USA* **88**, 5041–5045.
27. Chen, X. & Rubenstein, P.A. (1995) A mutation in an ATP-binding

loop of *Saccharomyces cerevisiae* actin (S14A) causes a temperature-sensitive phenotype *in vivo* and *in vitro*. *J. Biol. Chem.* **270**, 11406–11414.

28. Chen, X., Peng, J., Pedram, M., Swenson, C.E. & Rubenstein, P.A. (1995) The effect of the S14A mutation on the conformation and thermostability of *Saccharomyces cerevisiae* G-actin and its interaction with adenine nucleotides. *J. Biol. Chem.* **270**, 11415–11423.
29. Orlova, A., Chen, X., Rubenstein, P.A. & Egelman, E.H. (1997) Modulation of yeast F-actin structure by a mutation in the nucleotide-binding cleft. *J. Mol. Biol.* **271**, 235–243.
30. Wertman, K., Drubin, D.G. & Botstein, D. (1992) Systematic mutational analysis of the yeast ACT1 gene. *Genetics* **132**, 337–350.
31. Schüler, H., Korenbaum, E., Lindberg, U. & Karlsson, R. (1997) Studies on the ATP-binding site of actin using site-directed mutagenesis. In *Interacting Protein Domains: Their Role in Signal and Energy Transduction* (Heilmeyer, L., ed.), pp. 255–258. Springer-Verlag, Heidelberg.
32. Carlsson, L., Markey, F., Blikstad, I., Persson, T. & Lindberg, U. (1979) Reorganization of actin in platelets stimulated by thrombin as measured by the DNase I inhibition assay. *Proc. Natl Acad. Sci. USA* **76**, 6376–6380.
33. Kunkel, T.A., Roberts, T.T. & Zakour, R.A. (1987) Rapid and efficient site-specific mutagenesis without phenotypic selection. *Methods Enzymol.* **154**, 367–382.
34. Karlsson, R. (1988) Expression of chicken beta-actin in *Saccharomyces cerevisiae*. *Gene* **68**, 249–257.
35. Aspenström, P., Schutt, C.E., Lindberg, U. & Karlsson, R. (1993) Mutations in beta-actin: influence on polymer formation and on interactions with myosin and profilin. *FEBS Lett.* **329**, 163–170.
36. Lazarides, E. & Lindberg, U. (1974) Actin is the naturally occurring inhibitor of deoxyribonuclease I. *Proc. Natl Acad. Sci. USA* **71**, 4742–4746.
37. Houk, T.W. & Ue, K. (1974) The measurement of actin concentration in solution: a comparison of methods. *Anal. Biochem.* **62**, 66–74.
38. Gershman, L.C., Newman, J., Selden, L.A. & Estes, J.E. (1984) Bound-cation exchange affects the lag phase in actin polymerization. *Biochemistry* **23**, 2199–2203.
39. Lindberg, U., Schutt, C.E., Hellsten, E., Tjäder, A.-C. & Hult, T. (1988) The use of poly (L-proline)-Sepharose in the isolation of profilin and profilactin complexes. *Biochim. Biophys. Acta* **967**, 391–400.
40. Perry, S.V. (1955) Myosin adenosinetriphosphatase. *Methods Enzymol.* **2**, 582–588.
41. Laemmli, U.K. (1970) Cleavage of structural proteins during the assembly of the head of bacteriophage T4. *Nature* **227**, 680–685.
42. Gimona, M., Vandekerckhove, J., Goethals, M., Herzog, M., Lando, Z. & Small, J.V. (1994) Beta-actin specific monoclonal antibody. *Cell Motil. Cytoskeleton* **27**, 108–116.
43. Lehrer, S.S., Nagy, B. & Gergely, J. (1972) The binding of Cu^{2+} to actin without loss of polymerizability: the involvement of the rapidly reacting-SH group. *Arch. Biochem. Biophys.* **150**, 164–174.
44. Drabikowski, W., Lehrer, S.S., Nagy, B. & Gergely, J. (1977) Loss of Cu^{2+}-binding to actin upon removal of the C-terminal phenylalanine by carboxypeptidase A. *Arch. Biochem. Biophys.* **181**, 359–361.
45. Secrist, J.A., III, Barrio, J.R. & Leonard, N.J. (1972) A fluorescent modification of adenosine triphosphate with activity in enzyme systems: 1,N6-ethenoadenosine triphosphate. *Science* **175**, 646–647.
46. Waechter, F. & Engel, J. (1975) The kinetics of the exchange of G-actin-bound 1: *N*6-ethenoadenosine 5′-triphosphate with ATP as followed by fluorescence. *Eur. J. Biochem.* **57**, 453–459.
47. Spudich, J.A. (1974) Biochemical and structural studies of actomyosin-like proteins from non-muscle cells. II. Purification, properties and membrane association of actin from amoebae of *Dictyostelium discoideum*. *J. Biol. Chem.* **249**, 6013–6020.
48. Blikstad, I., Markey, F., Carlsson, L., Persson, T. & Lindberg, U. (1978) Selective assay of monomeric and filamentous actin in cell extracts, using inhibition of deoxyribonuclease I. *Cell* **15**, 935–943.
49. Conejero-Lara, F., Mateo, P.L., Aviles, F.X. & Sanchez-Ruiz, J.M. (1991) Effect of Zn^{2+} on the thermal denaturation of carboxypeptidase B. *Biochemistry* **30**, 2067–2072.
50. Kouyama, T. & Mihashi, K. (1981) Fluorimetry study of *N*-(1-pyrenyl) iodoacetamide-labelled F-actin. Local structural change of actin protomer both on polymerization and on binding of heavy meromyosin. *Eur. J. Biochem.* **114**, 33–38.
51. Kron, S.J. & Spudich, J.A. (1986) Fluorescent actin filaments move on myosin fixed to a glass surface. *Proc. Natl Acad. Sci. USA* **83**, 6272–6276.
52. Kishino, A. & Yanagida, T. (1988) Force measurements by micromanipulation of a single actin filament by glass needles. *Nature* **334**, 74–76.
53. Gorbunoff, M.J. & Timasheff, S.N. (1984) The interaction of proteins with hydroxyapatite. III. Mechanism. *Anal. Biochem.* **136**, 440–445.
54. Malm, B. (1984) Chemical modification of Cys-374 of actin interferes with the formation of the profilactin complex. *FEBS Lett.* **173**, 399–402.
55. Le Bihan, T. & Gicquaud, C. (1993) Kinetic study of the thermal denaturation of G actin using differential scanning calorimetry and intrinsic fluorescence spectroscopy. *Biochem. Biophys. Res. Comm.* **194**, 1065–1073.
56. Aspenström, P., Engkvist, H., Lindberg, U. & Karlsson, R. (1992) Characterization of yeast-expressed beta-actins, site-specifically mutated at the tumor-related residue Gly245. *Eur. J. Biochem.* **207**, 315–320.
57. Selden, L.A., Estes, J.E. & Gershman, L.C. (1983) The tightly bound divalent cation regulates actin polymerization. *Biochem. Biophys. Res. Comm.* **116**, 478–485.
58. Frieden, C. & Patane, K. (1988) Mechanism for nucleotide exchange in monomeric actin. *Biochemistry* **27**, 3812–3820.
59. Selden, L.A., Kinosian, H.J., Estes, J.E. & Gershman, L.C. (1999) Impact of profilin on actin-bound nucleotide exchange and actin polymerization dynamics. *Biochemistry* **38**, 2769–2778.
60. Geffrey, G.A. & Sanger, W. (1994) *Hydrogen Bonding in Biological Structures*. Springer-Verlag, Heidelberg.
61. Creighton, T.E. (1993) *Proteins: Structures and Molecular Properties*, 2nd edn. W. H. Freeman, New York, USA.
62. Stuckey, J.A., Schubert, H.L., Fauman, E.B., Zhang, Z.-Y., Dixon, J.E. & Saper, M.A. (1994) Crystal structure of *Yersinia* protein tyrosine phosphatase at 2.5 Å and the complex with tungstate. *Nature* **370**, 571–575.
63. Su, X.-D., Taddei, N., Stefani, M., Ramponi, G. & Nordlund, P. (1994) The crystal structure of a low-molecular-weight phosphotyrosine protein phosphatase. *Nature* **370**, 575–578.
64. Schnetz, K., Sutrina, S.L., Saier, M.H. Jr. & & Rak, B. (1990) Identification of catalytic residues in the beta-glucoside permease of *Escherichia coli* by site-specific mutagenesis and demonstration of interdomain cross-reactivity between the beta-glucoside and glucose systems. *J. Biol. Chem.* **265**, 13464–13471.
65. van Montford, R.L.M., Pijning, T., Kalk, K.H., Reizer, J., Saier, M.H., Jr., Thunnissen, M.M.G.M., Robillard, G.T. & Dijkstra, B.W. (1997) The structure of an energy-coupling protein from bacteria, IIBcellobiose, reveals similarity to eukaryotic protein tyrosine phosphatases. *Structure* **5**, 217–225.
66. Fisher, A.J., Smith, C.A., Thoden, J.B., Smith, R., Sutoh, K., Holden, H.M. & Rayment, I. (1995) X-ray structures of the myosin motor domain of *Dictyostelium discoideum* complexed with MgADP.BeF_x and MgADP.AlF_4. *Biochemistry* **34**, 8960–8972.
67. O'Brien, M.C., Flaherty, K.M. & McKay, D.B. (1996) Lysine 71 of the chaperone protein Hsc70 Is essential for ATP hydrolysis. *J. Biol. Chem.* **271**, 15874–15878.
68. Wilbanks, S.M. & McKay, D.B. (1995) How potassium affects the activity of the molecular chaperone Hsc70. II. Potassium binds specifically in the ATPase active site. *J. Biol. Chem.* **270**, 2251–2257.
69. Schweins, T., Geyer, M., Scheffzek, K., Warshel, A., Kalbitzer, H.R. & Wittinghofer, A. (1995) Substrate-assisted catalysis as a mechanism for GTP hydrolysis of p21ras and other GTP-binding proteins. *Nat. Struct. Biol.* **2**, 36–44.
70. Smith, C.A. & Rayment, I. (1996) Active site comparisons highlight

structural similarities between myosin and other P-loop proteins. *Biophys. J.* **70**, 1590–1602.

71. Sprang, S.R. (1997) G proteins, effectors and GAPs: structure and mechanism. *Curr. Opin. Struct. Biol.* **7**, 849–856.
72. Stock, A.M., Martinez-Hackart, E., Rasmussen, B.F., West, A.H., Stock, J.B., Ringe, D. & Petsko, G.A. (1993) Structure of the Mg (2+)-bound form of CheY and mechanism of phosphoryl transfer in bacterial chemotaxis. *Biochemistry* **32**, 13375–13380.
73. Gordon, D.J., Boyer, J.L. & Korn, E.D. (1977) Comparative biochemistry of non-muscle actins. *J. Biol. Chem.* **252**, 8300–8309.
74. Hitchcock, S.E., Carlsson, L. & Lindberg, U. (1976) Depolymerization of F-actin by deoxyribonuclease I. *Cell* **7**, 531–542.